



Biocatalytic and biological activities of *Kigelia africana* mediated silver monometallic and copper-silver bimetallic nanoparticles

Buyani Biyela & Viresh Mohanlall*

Department of Biotechnology and Food Technology, Faculty of Applied Sciences, Durban University of Technology, Durban-4001, South Africa

Received 06 July 2020; revised 08 January 2022

Aqueous extract of *Kigelia africana* leaves have been utilized for the synthesis of silver (AgNPs) and copper-silver bimetallic nanoparticles (Ag-CuNPs) that were generally found to be spherical and oval in shape. The synthesized nanoparticles were characterized using UV-Vis, Fourier-transform infrared spectroscopy (FTIR), scanning electron microscopy/energy dispersive X-ray analysis (SEM/EDX), and transmission electron microscopy (TEM). The antimicrobial activities were evaluated against both gram-negative and gram-positive strains of bacteria. The UV-Vis and FTIR techniques revealed the formation of nanoparticles and the active components were adsorbed on the surface of the particles thereby stabilizing the nanoparticles. The SEM reveals uniform microspheres of AgNPs and anisotropic particles for Ag-CuNPs. TEM shows the size of synthesized particles. The nanoparticles inhibited the growth of both gram-negative and gram-positive bacteria. The bimetallic nanoparticles synthesized from aqueous extract of *K. africana* leaves showed greater inhibition against *Escherichia coli* as compared to the monometallic nanoparticles. The AgNPs were more effective for the reduction of 4-nitrophenol and 4-nitroaniline as compared to Ag-CuNPs. The results of this study confirmed that *Kigelia africana* leaf and fruit aqueous extract can successfully reduce metallic ions to synthesize metallic nanoparticles that have antimicrobial and biocatalytic properties.

Keywords: Bimetallic nanoparticles, Biocatalytic agents, *Kigelia africana*

Modern health has been negatively affected globally by the increase in antimicrobial resistance. Antimicrobial resistance to an array of different categories of antibiotics can be due to the irresponsible habits of antibiotic prescription. Thus, the assumption that is obtained as the derivation from this phenomenon is the impact in future efficacy and usage of drugs within both community and hospital care globally¹. Nanotechnology is one of the several strategies that can be used to overcome antibiotic drug resistance, this is due to the fact that nanotechnology allows the synthesis of nano-sized molecules or particles also known as nanoparticles².

Nanoparticles are the fundamental core of nanotechnology, their size range is between 1 and 100 nanometers and is made of carbon, metal, metal oxides or organic matter³. In addition, nanoparticles can be applied not only for the overcoming of antibiotic resistance, but their applications can be extended for both biological and environmental researchers in so many different fields. This includes

the detection of biomolecules, substrate coding, signal transduction and amplification, microbial monitoring and detection, chemical degradation and source recovery⁴. Nanoparticles are attractive for different applications or industries because they have important and unique features, such as surface to mass ratio that is much larger than that of other particles, their quantum properties and their ability to carry and adsorb to other compounds. In addition, their large surface is functional, and it enables the binding, adsorption, and carrying of other compounds such as drugs, probes and proteins⁵. There are different types of nanoparticles which include carbon nanotubes, dendrimer nanomaterials, liposome nanoparticles, polymeric nanoparticles and metallic nanoparticles⁶.

There are two most popular approaches that are used to synthesize nanoparticles. Firstly, there is a chemical approach which includes the chemical reduction using different kinds of organic and inorganic reducing agents, however, this approach is considered not to be environmental-friendly. Secondly, there is a biological method which is known to be eco-friendly, this method falls under green synthesis approaches, and it can include the use

*Correspondence:
E-mail: vireshm55@gmail.com

of biological systems to aid in the synthesis and stabilizing of nanoparticles⁷.

This study focuses on the green synthesis of copper-silver bimetallic nanoparticles using *Kigelia africana*. The copper-silver bimetallic nanoparticles were then characterized using UV-Vis and FTIR spectroscopy, Scanning Electron Microscopy with Energy Dispersive Absorption X-ray (EDAX) spectroscopy and Transmission Electron Microscopy. The biological activity against gram negative and gram-positive organisms and biocatalytic activity against nitrophenol and nitroalanine was then evaluated.

Experimental

Materials

Mueller Hinton Agar plates, Microtiter plates and Mueller Hinton Broth (MHB) were purchased from Bio-Rad Laboratories (Richmond, VA, USA). Bacterial cultures were obtained from Lancet Laboratories (SA). Microbank vials were purchased from Davies diagnostic, (SA). All chemicals were of analytical grade and were supplied by Sigma-Aldrich (St Louis, MO, USA).

Methods

Plant extract preparation

Leaf extract

The leaves of *K. africana* were harvested from the Steve Biko Campus, Durban University of Technology, Durban, South Africa. The leaves were washed thoroughly and cut. The leaves were air-dried. Leaf (20 g) was mixed with distilled water (100 mL) and the mixture was heated at 60°C while stirring for 20 min. The resultant mixture was filtered, and the filtrate stored at 4°C.

Synthesis of nanoparticles

Silver (Ag) monometallic nanoparticles

Four millimolar of silver nitrate (AgNO_3) was prepared and used for the synthesis of silver monometallic nanoparticles. 1 mL of plant extract was added into 24 mL of prepared aqueous solution of silver nitrate for reduction to Ag^+ ions and kept at 80°C for six h. Six portions of 1 mL of the mixture were removed from the reaction vessel after every 1 hour, the reaction stopped after 6 h. The products were then centrifuged at 11000 rpm for 30 min, and dried at 50°C and stored in an airtight container for further analysis.

Silver (Ag) + Copper (Cu) bimetallic nanoparticles

A well-mixed aqueous solution of AgNO_3 (0.5 mM) and $\text{CuCl}_2 \cdot 2\text{H}_2\text{O}$ (0.5 mM) was prepared.

The leaf extract of *K. africana* (90 mL) was mixed with the bimetallic solution with gently stirring using a magnetic stirrer at 100°C for 6 h. The formation of nanoparticles was represented by the change in colour from light brown to dark brown. Six portions of 1 mL of the mixture were removed from the reaction vessel after every 1 h, the reaction stopped after 6 h. The products were then centrifuged at 11000 rpm for 30 min and dried at 50°C and stored in an airtight container for further analysis.

Characterization of the Synthesized Nanoparticles

Ultra-Violet (UV) Spectroscopy

The formation and stability of the monometallic AgNPs and bimetallic Ag-CuNPs were analysed by UV-Visible spectroscopy using a Varian Cary 100 UV-Vis spectrophotometer with Win UV software. A scan in the wavelength range of 200 to 800 nm was carried out. Samples were poured into quartz cuvettes, placed into the spectrophotometer and a scan in the wavelength range of 200 to 800 nm was carried out. Thereafter, the absorbance measurements in relative light units (AU) were recorded.

Transmission Electron Microscopy (TEM)

TEM was used to determine the morphology and particle size of the synthesized monometallic AgNPs and bimetallic Ag-CuNPs. Five milligrams of the powdered sample of the monometallic AgNPs and bimetallic Ag-CuNPs were redispersed from the powdered form using ethanol and then sonicated for 15 min. From this, a drop of each sample was then placed on a carbon-coated copper grid and allowed to air dry at room temperature before loading into the Transmission Electron Microscope for analysis. The microscope used was a JEOL JEM-1010 Transmission Electron Microscope with a Megaview III camera and iTEM UIP software (Tokyo, Japan) accessed from the University of Kwa-Zulu Natal (Westville Campus, South Africa).

Scanning Electron Microscopy (SEM) And Energy Dispersive X-Ray Analysis (EDX)

To investigate the presence of silver and copper nanoparticles and for the particle image, a drop of the monometallic AgNPs and bimetallic Ag-CuNPs were placed on an aluminium stub, and then allowed to air dry, this permits the water to evaporate and be viewed using a ZEISS LEO 1450 Scanning electron microscope (conventional SEM and X-ray microanalysis) at the University of Kwa-Zulu Natal. For elemental analysis, the nanoparticles

were subjected to energy dispersive X-Ray analysis coupled to SEM.

Fourier-Transform Infrared (FTIR) Spectroscopy

FTIR analyses were also used to identify the biomolecules that were responsible for the synthesis and capping of the monometallic AgNPs and bimetallic Ag-CuNPs for the different extracts. At the onset, sample preparations involved centrifugation of monometallic AgNPs and bimetallic Ag-CuNPs solutions at 1300 rpm for 45 min, followed by discarding of the supernatant, and re-suspending of the precipitants in distilled water. From this, a drop of the sample was then placed on a Perkin Elmer, Spectrum 100 FTIR spectrophotometer and a scan measuring transmittance percentage over the range of wave numbers from 400 to 4000 cm^{-1} was taken. Thereafter, E-FTIR software was used to analyze the results and as certain peak values which were then interpreted.

Catalytic Reduction of 4-Nitrophenol and 4-Nitroaniline

The synthesized AgNPs and bimetallic Ag-CuNPs were used as catalyst for the reduction of nitro-organic compounds, 4-nitrophenol and 4-nitroaniline to amino compounds by sodium borohydride⁸. To a 3 mL cuvette containing freshly prepared sodium borohydride (1 mL, 0.2 M) solution, 4-nitrophenol (1.7 mL, 0.2 mM) solution was added. The cuvette was then placed in a UV-Vis spectrophotometer and the absorbance against wavelengths recorded. After adding metal nanoparticles (0.1 mL, 0.1%) solution, the cuvette was shaken vigorously for mixing and kept in a UV-Vis spectrophotometer and scanned from 200 to 800 nm ranges. The same protocol was followed for reduction of 4-nitroaniline.

Antibacterial activity of the AgNPs and Ag-CuNPs

Synthesized AgNPs and bimetallic Ag-CuNPs were tested for antimicrobial activity by disc diffusion method against pathogenic bacteria, *Klebsiella pneumonia* (ATCC 70603), *Pseudomonas aeruginosa* (ATCC 27853), *Bacillus cereus* (ATCC 10876), *Enterococcus faecalis* (ATCC 29212), *Staphylococcus aureus* (ATCC 25923) and *Escherichia coli* (ATCC 25922). The sterilized discs were dipped in different concentrations of silver nanoparticle dispersion in dimethyl sulfoxide (DMSO), namely, 100% (1000 $\mu\text{g/mL}$), 50% (500 $\mu\text{g/mL}$), and 25% (250 $\mu\text{g/mL}$), and dried in an oven at 30–40°C. The AgNPs and bimetallic Ag-CuNPs impregnated discs were placed on the plates and kept for incubation at

37°C for 24 h. After incubation, the different levels of zone of inhibition of bacteria were measured. The standard antibiotic drug, Ciprofloxacin was used as a positive control and 10% DMSO was used as a negative control. The experiments were done in triplicate and mean values of zone diameter were recorded in millimetres.

Statistical analysis

Antibacterial activity studies were performed in triplicate and the results expressed as mean \pm standard deviation (S.D). Data analyzed by two-way ANOVA and *t*-test using GraphPad Prism 6.0 and statistically significant values are indicated by $P < 0.5$.

Results and Discussion

Synthesis of AgNPs, UV-Vis Spectroscopy SEM and TEM Analysis

Metal nanoparticles are well known for their unique properties, particularly, optical, as a result of surface plasmon resonance (SPR). Thus, the successful formation of AgNPs and bimetallic Ag-CuNPs was confirmed with colour change and UV-Vis spectroscopy.

The AgNPs and bimetallic Ag-CuNPs were prepared by mixing plant leaf extracts of *K. africana* with AgNO_3 and $\text{CuCl}_2 \cdot 2\text{H}_2\text{O}$ solutions. This synthesis of the silver monometallic nanoparticles was indicated by the colour change of the reaction mixture from yellow to dark orange solution (Fig. 1A). This synthesis of the bimetallic Ag-CuNPs was indicated by the colour change of the reaction mixture from yellow to a dark brown solution (Fig. 1B). The colour change can be attributed to the reduction of silver (Ag^+) and copper ions (Cu^{2+}) from silver nitrate and copper chloride respectively into AgNPs by active biomolecules present in the plant extract⁹.

The UV-Vis absorption spectra show absorption maxima in the range of 460 nm for mono metallic silver nanoparticles (AgNPs) and 280 nm for the bimetallic silver-copper nanoparticles (AgCuNPs) from *K. africana* leaf extracts (Fig. 2). Studies by Daghestani and Day

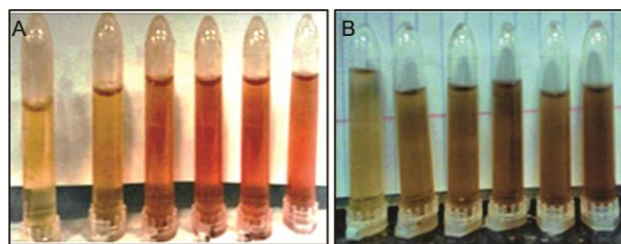


Fig. 1 — Positive colour change for aqueous leaf extract with monometallic AgNO_3 (0.5 mM) solution (A), bimetallic AgNO_3 (0.5 mM) and $\text{CuCl}_2 \cdot 2\text{H}_2\text{O}$ (0.5 mM) solutions (B) after 6 h

(2014)¹⁰ indicated that the surface plasmon resonance arising from the interactions of the electron cloud on the particles' surface and the electromagnetic radiation is in the range of 380 to 480 nm. The absorption bands for the bimetallic nanoparticles in the range 280 to 320 nm range is a clear indication of reductive metabolites in the *K. africana* fruit extract. This represents a discrete nucleation event with secondary metabolites of the

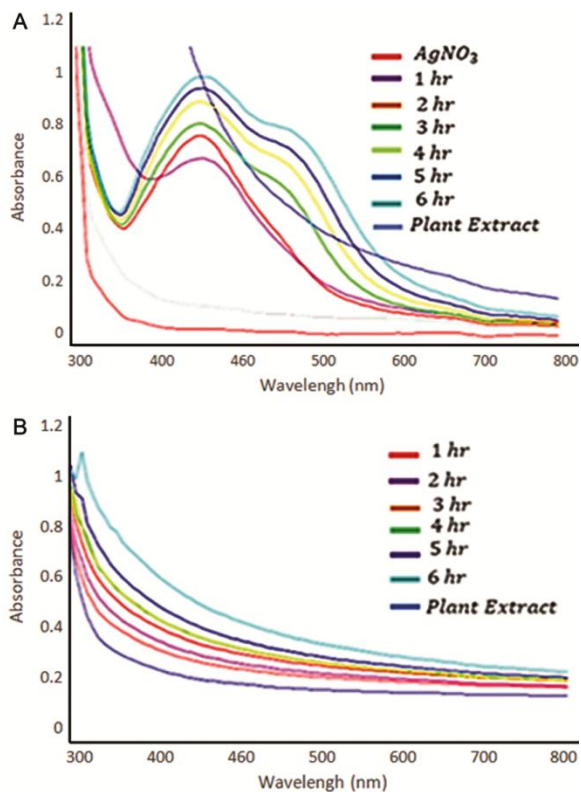


Fig. 2 — UV-Vis absorption spectra of synthesized (A) monometallic silver nanoparticles (AgNPs); and (B) bimetallic silver-copper nanoparticles (AgCuNPs) from *K. africana* leaf extracts

extract being adsorbed on the surface of the nanoparticles¹¹.

SEM micrographs of the synthesized AgNPs and bimetallic Ag-CuNPs of *K. africana* magnified at $\times 50\,000$ - $\times 100\,000$ and measured at 200 and 100 nm are shown in (Fig. 3). Leaf AgNPs showed monodisperse microspheres and AgCuNPs showed anisotropic microplates. Elemental composition analysis using Energy Dispersive X-Ray Analysis (EDX) demonstrates the chemical purity of the synthesized AgNPs and AgCuNPs (Figs 4 & 5). The elemental analysis of the AgNPs shown in the figure revealed a strong silver signal (74.91%) along with weak signals of O (3.12%), Cl (10.96%) and C (11.01%). The energy dispersive X-ray scans of both monometallic and bimetallic nanoparticles showed the presence of carbon, oxygen, chlorine, potassium, calcium and nitrogen originating from the secondary metabolites in the plant extract which acts as stabilizers. The energy dispersive X-ray scans of monometallic nanoparticles reflected a peak around 3.0 KeV which corresponds to the binding energies of leaf AgNPs. The intensity of the peak was reduced in the case of leaf bimetallic nanoparticles (AgCuNPs) with additional copper peaks about 1.0, 8.0, and 9.0 KeV. The SEM and EDX results are in agreement to research conducted by Ashishie *et al.* (2018)¹² who

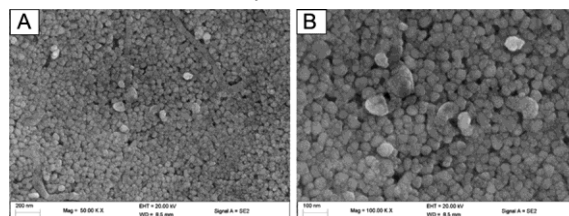


Fig. 3 — SEM micrograph of synthesized AgNPs at (A) 50 000 X; and (B) 100 000 X magnification

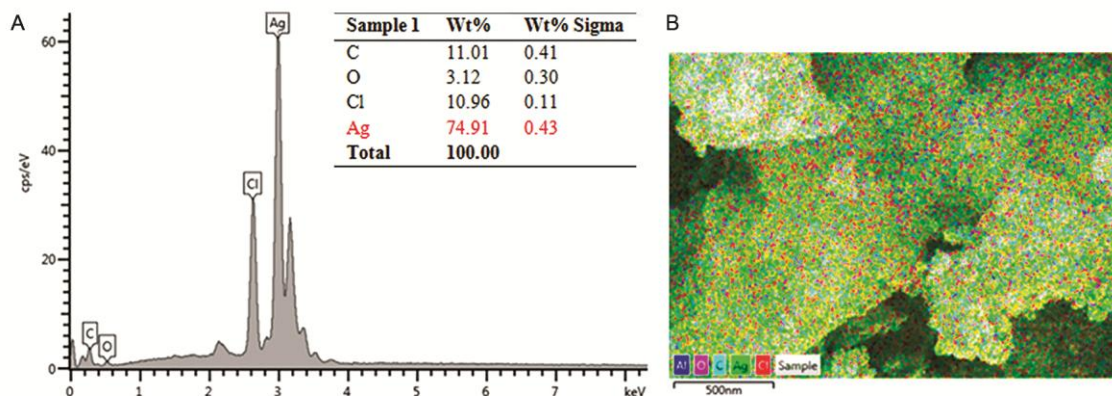


Fig. 4 — (A) Elemental composition of AgNPs using Scanning Electron Microscopy (SEM) and Energy Dispersive X-Ray Analysis (EDX), and (B) Elemental map showing the presence of Aluminium, Oxygen, Carbon, Silver and Chlorine

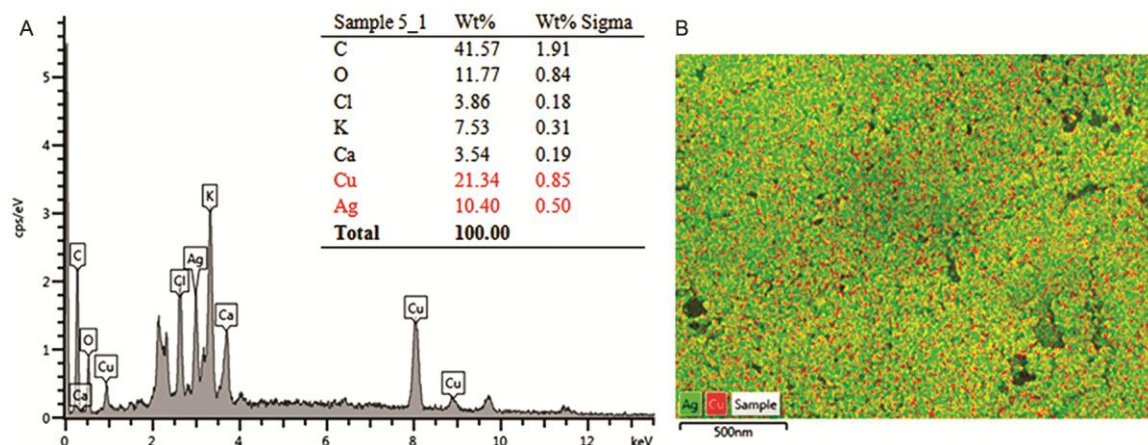


Fig. 5 — (A) Elemental composition of bimetallic Ag-CuNPs of *K. africana* using Scanning Electron Microscopy (SEM) and Energy Dispersive X-Ray Analysis (EDX); and (B) Elemental map showing the presence of copper and silver

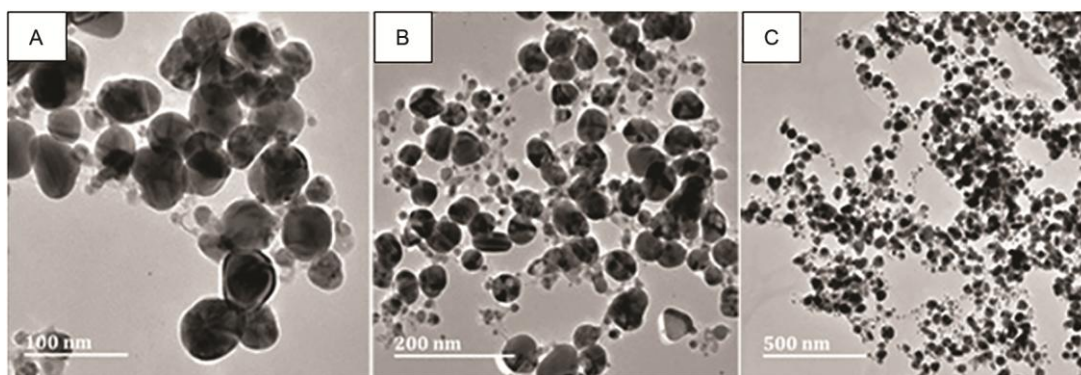


Fig. 6 — TEM micrograph of AgNPs using *K. africana* at the scale bar corresponding to (A) 100 nm; (B) 200 nm; and (C) 500 nm scale

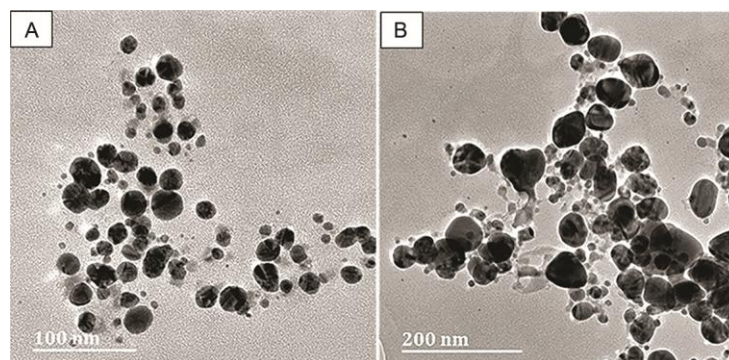


Fig. 7 — TEM micrograph of Ag-CuNPs of *K. africana* at the scale bar corresponding to (A) 100 nm; and (B) 200 nm scale

reported that the weight percent of silver is 80.64 and 8.69, respectively, for AgNPs and AgCuNPs.

Figures 6 & 7 shows the TEM micrographs of leaf AgNPs and AgCuNPs, respectively. The nanoparticles were observed to be in the size range of 10-20 nm. In terms of shapes, leaf AgNPs were observed to be spherical, whilst AgCuNPs were observed to be a combination of spheres and rods.

FTIR analysis

FTIR measurements were carried out to identify the major functional groups on the surface of the plant extract and its possible involvement in the capping and stabilization of the AgNPs. In Figure 8, FTIR spectra of AgNPs show strong absorption band at 1600 cm^{-1} and it is attributed to binding of NHC=O to metal ions. Other peaks of interest

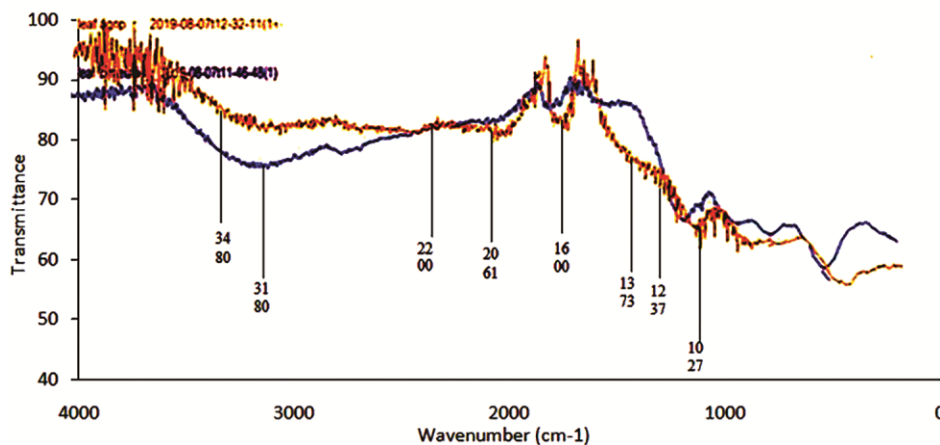


Fig. 8 — FTIR spectra of aqueous leaf extract of *K. africana* Ag-CuNPs (blue) and AgNPs (orange)

include 2922 cm^{-1} (secondary amine), 1373 cm^{-1} (C-N stretching vibration of aromatic amine), 1237 cm^{-1} and 1027 cm^{-1} for AgNPs in aqueous *K. africana* leaf extracts. The presence of peaks at 3180 cm^{-1} and 3480 cm^{-1} could be due to O-H group in polyphenols or proteins or polysaccharide^{13,14}. The phytochemical analysis of aqueous *K. africana* has indicated the presence of phenolic compounds and iridoids such as caffeic acid, ferulic acid, p-coumaric acid, caffeic acid glucoside, p-coumaroyl glucoside, verminoside and specioside which are responsible for the formation of metal nanoparticles. The presence of amide and carboxylic acid bonds in both samples confirmed the presence of protein polymers in the leaf extract which could be involved in the reduction of Ag^+ to Ag^0 . Biomolecules are known to interact with metal salts *via* these functional groups and aid their reduction to NPs¹⁵.

Biocatalytic reduction of nitroorganic compounds

Reduction reactions for 4-nitrophenol (4-NP) and 4-nitroalanine (4-NA) using aqueous NaBH_4 is thermodynamically favourable. However, the presence of the kinetic barrier due to large potential difference between donor and acceptor molecules decreases the feasibility of this reaction. AgNPs overcome the kinetic barrier by by facilitating electron relay from the donor BH_4^- to acceptor 4-NP/4-NA. In the presence of AgNPs as a catalyst, the yellow colour of 4-NP solution gradually became clear and finally disappeared. In Figure 9A, the UV-Vis absorption spectra revealed that the addition of AgNPs initiated the lowering of peak intensity at 400 nm and the presence of a new absorption peak at 280 nm indicating the formation of 4-aminophenol. The complete disappearance of the 400 nm peak was observed within 30 min. The silver nanoparticles

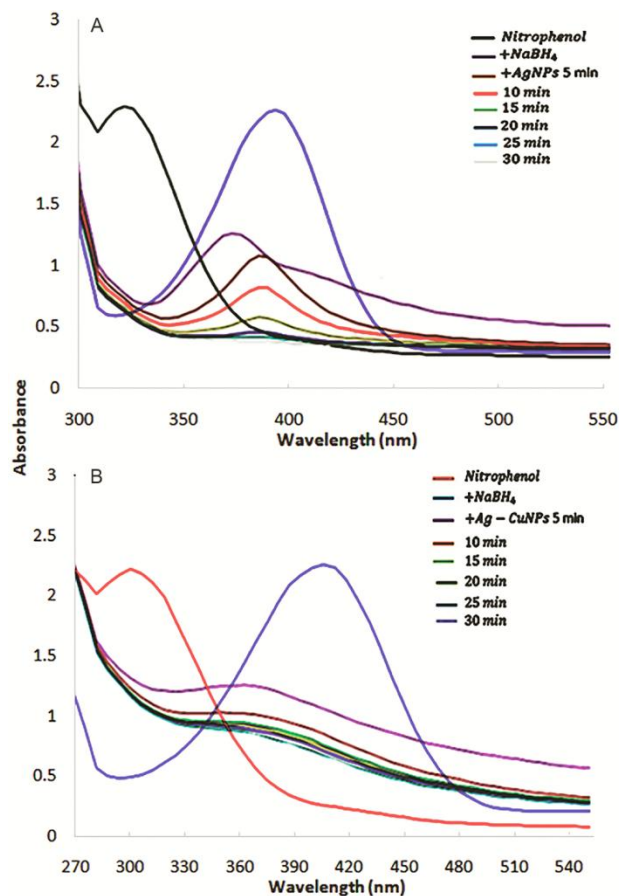


Fig. 9 — (A & B) UV-Vis spectrum of the reduction of 4-nitrophenol (4-NP) by *K. africana*/AgNP conjugates

showed better reduction after 30 min when compared to silver-copper nanoparticles, this may be due to the high agglomeration in bimetallic nanoparticles, thus not providing enough surface area for 4-NP and NaBH_4 to exchange electrons for the reduction to 4-aminophenol (Fig. 9B).

The reduction reaction of 4-NA was monitored by UV-Vis spectroscopy by measuring the decrease in the absorbance intensity at 380 nm. The reduction reaction of 4-NA by NaBH_4 did not take place in the absence of the AgNPs and Ag-CuNPs as shown in (Fig. 10) but after the addition of the NPs, immediate reduction took place. This reduction was also observed visually by the steady disappearance of the yellow colour. The reduction reaction was monitored every 5 min using UV-Vis spectroscopy.

In the process of biocatalytic reduction, NaBH_4 acts as electron donor and hydrogen supplier, the AgNPs and Ag-CuNPs are an electron transfer mediator that collect electrons from BH_4^- ion to 4-NP and 4-NA¹⁶. The simultaneous adsorption of hydrogen species from BH_4^- , 4-NP and 4-NA on the surface of AgNPs and Ag-CuNPs takes place and diffusion between the adsorbed species leads to desorption of the product¹⁷. The complete reduction of 4-NA results in the formation of 1,4-diaminobenzene after 30 min.

Antibacterial activity

AgNPs are well known for their antimicrobial activity, which is said to be attributed to the electrostatic

interaction that occurs between the negatively charged cell membrane of microorganism and the positively charged AgNPs¹⁸. The accumulation of AgNPs on the cell membrane is believed to alter the membrane causing it to lose permeability which leads to cell death¹⁹. However, due to chemical agents used when preparing these NPs which affect their biocompatibility and pose environmental problems, biosynthesized AgNPs have been the subject of research recently.

Dimethylsulfoxide (DMSO) was used as a negative control and also proved to be a safe solvent, which offered no interference with the results obtained in the assay. The diameter of inhibition zones (mm) around each well with AgNPs and AgCuNPs solutions is presented in (Table 1). Synthesized AgNPs exhibited good antimicrobial activity against both gram-positive and gram-negative bacteria, with varying degrees of inhibition (Table 1). *S. aureus* had a slightly larger zone of inhibition (9 mm) as compared to the other bacterial strains. Overall, these findings revealed that good antibacterial activity was achieved at higher doses of the *K. africana* mediated AgNPs and AgCuNPs against all tested bacterial strains,

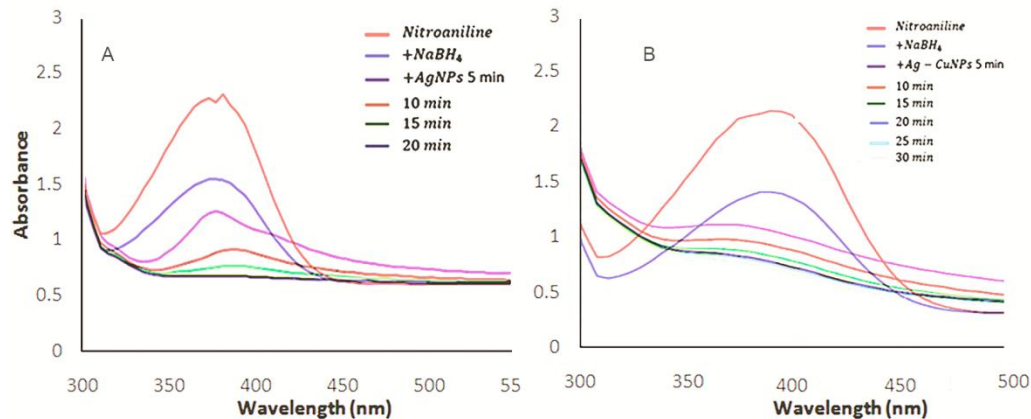


Fig. 10 — UV-Vis spectra of the catalytic reduction of 4-Nitroaniline to 4-phenylenediamine using *K. africana* (A) AgNPs; and (B) Ag-CuNP conjugates

Table 1 — Antibacterial activity of *K. africana*/AgNPs and Ag-CuNP conjugates

| | AgNP 1000µg/mL | AgNP 500 µg/mL | AgNP 250 µg/mL | Ag-CuNP 1000 µg/mL | Ag- CuNP500 µg/mL | Ag- CuNP250 µg/mL | + control* | AgNO ₃ | AgNO ₃ + CuCl ₂ .2H ₂ O |
|----------------------|-------------------|-------------------|-------------------|-----------------------|-------------------------|-------------------------|------------|-------------------|---|
| Bacteria | | | | | | | | | |
| <i>E. coli</i> | 8 ± 0.1 | 6 ± 0.1 | 6 ± 0.1 | 6 ± 0.1 | 5 ± 0.1 | 4.2±0.1 | 35 ± 0.2 | 4 ± 0.2 | 3 ± 0.1 |
| <i>K.pneumoniae</i> | 4.2 ± 0.2 | 4.2 ± 0.2 | 4 ± 0.1 | 4 ± 0.1 | 4 ± 0.1 | 4±0.1 | 20 ± 0.3 | 4 ± 0.1 | 3 ± 0.3 |
| <i>P. aeruginosa</i> | 5 ± 0.2 | 5 ± 0.1 | 4 ± 0.1 | 4 ± 0.1 | 4 ± 0.1 | 4±0.1 | 15 ± 0.5 | 3 ± 0.2 | 3 ± 0.1 |
| <i>S. aureus</i> | 9 ± 0.2 | 6 ± 0.2 | 5 ± 0.1 | 5 ± 0.1 | 4 ± 0.1 | NA | 26 ± 0.1 | 4 ± 0.1 | 3 ± 0.1 |
| <i>B. cereus</i> | 5.8 ± 0.1 | 5 ± 0.1 | 4.3±0.1 | 5 ± 0.1 | 4.5 ± 0.1 | 4.1±0.1 | 22.5 ± 0.5 | 4 ± 0.2 | 4 ± 0.2 |
| <i>E. faecalis</i> | 5 ± 0.1 | 4.3 ± 0.3 | NA | 4.2±0.1 | NA | NA | 26 ± 0.1 | 4 ± 0.1 | 3 ± 0.3 |

* - Ciprofloxacin

NA – no activity

suggesting that *K. africana* mediated AgNPs and AgCuNPs were good antimicrobial agents. The monometallic AgNPs showed a distinct increase in antibacterial activity as compared to the bimetallic AgCuNPs.

The results revealed that AgNPs with a positive surface charge was the most effective against all types of bacteria (gram-negative and gram-positive), however AgCuNPs with a negative surface charge is the least effective against the bacteria²⁰. AgNPs in general have many mechanisms for causing cell death. AgNPs are able to cause cell death by being absorbed into the cells, once in the cell it induces DNA damage and subsequently cell death²¹. According to Brunner *et al.* (2006)²² the toxicity of AgNPs may be due to the direct interaction with the nanoparticles and the biological macromolecules or the release of metal ions from the nanoparticle. Using direct interaction, the NPs anchor themselves to the bacterial cell wall. This subsequently causes the cell wall to break apart and the nanoparticle can infiltrate the cell. Due to the membrane break, contents of the cell tend to leak out of the cell membrane and this can cause cell death²³. When the nanoparticles enter the cell it may interact with cellular components such as proteins, lipids and DNA, this interaction leads to dysfunction and death of the cell. An example is the interaction between the ribosomes and the nanoparticles, the ribosomes become denatured and this in turn inhibits translation as well as protein synthesis. Another antibacterial mechanism involves the production of high levels of reactive oxygen species (ROS), such as hydroxyl radical, hydrogen peroxide, hypochlorous acid and superoxide anion. This ROS generated in excess in the cell leads to inhibition of respiration and inhibition of cell growth²¹.

Conclusion

AgNPs and AgCuNPs were successfully synthesized using leaf extracts of *K. africana*. The metal nanoparticles were characterized by UV-Vis, SEM-EDX, TEM and FTIR measurements. The formation of AgNPs and AgCuNPs was observed by visible color change from yellow to brown/red and was confirmed by UV-Visible spectroscopy. These AgNPs and AgCuNPs were very stable, and showed antibacterial activity against a range of tested gram-positive and gram-negative bacteria at low doses, thus proving to be good antimicrobial agents. The AgNPs and AgCuNPs have increased catalytic ability for the reduction of 4-NP and 4-NA after a 30 min time interval. This research augments the application of green synthesized

nanoparticles over chemically synthesized nanoparticles for the bioremediation of nitro organic waste in wastewater systems.

Acknowledgement

The National Research Foundation of South Africa and the Durban University of Technology are acknowledged for financial and infrastructural support.

Conflicts of interest

All authors declare no conflict of interests.

References

- 1 Kumar M, Curtis A & Hoskins C, Application of nanoparticle technologies in the combat against anti-microbial resistance. *Pharmaceutics*, 10 (2018) 11.
- 2 Rudramurthy GR, Swamy MK, Sinniah UR & Ghasemzadeh A, Nanoparticles: Alternatives against drug-resistant pathogenic microbes. *Molecules*, 21 (2016) 836
- 3 Ealias AM & Saravanakumar MP, A review on the classification, characterisation, synthesis of nanoparticles and their application. *Mater Sci Eng C*, 263 (2017) 032019.
- 4 Liu W, Nanoparticles and Their Biological and Environmental Applications. *J Biosci Bioeng*, 102 (2006) 1.
- 5 Shukla S, A Review Article on Nanoparticle. *Pharmatutor*, 7 (2019).
- 6 Bhatia S, Nanoparticles types, classification, characterization, fabrication methods and drug delivery applications. *Natl Polym Drug Deliv Syst*, (2016) 33.
- 7 Irvani S, Korbekandi H, Mirmohammadi SV & Zolfaghari B, Synthesis of silver nanoparticles: chemical, physical and biological methods. *Res Pharm Sci*, 9 (2014) 385.
- 8 Pradhan N, Pal A & Pal T, Silver nanoparticle catalyzed reduction of aromatic nitro compounds. *Colloids Surf A Physicochem Eng Asp*, 196 (2002) 247.
- 9 Jain A, Rapid Green Synthesis of Silver Nanoparticles (AgNPs) using (*Prunus persica*) Plants extract: Exploring its Antimicrobial and Catalytic Activities. *Int J Nanomed Nanotechnol*, 8 (2017) 2157.
- 10 Daghestani HN & Day BW. Theory and applications of surface plasmon resonance, resonant mirror, resonant waveguide grating, and dual polarization interferometry biosensors. *Sensors*, 10 (2010) 9630.
- 11 Mobark R, Mohammed O, Tajelseir K & Mustafa O, Phytochemical investigation of antimicrobial activities leaves extract of *Kigelia africana*. *Biol Chem Res*, 3 (2015) 44.
- 12 Ashishie PB, Anyama CA, Ayil AA, Oseghale CO, Adesujand ET & Labulo AH, Green synthesis of silver monometallic and copper-silver bimetallic nanoparticles using *Kigelia africana* fruit extract and evaluation of their antimicrobial activities. *Int J Phys Sci*, 13 (2018) 24.
- 13 Song JY, Jang H-K & Kim BS, Biological synthesis of gold nanoparticles using *Magnolia kobus* and *Diopyros kaki* leaf extracts. *Process Biochem*, 44 (2009)1133.
- 14 Susanto H, Feng Y & Ulbricht M, Fouling behavior of aqueous solutions of polyphenolic compounds during ultrafiltration. *J Food Eng*, 91 (2009) 333.
- 15 Hamouda RA, Hussein MH, Rasha AA & Bazawir SS, Synthesis and biological characterization of silver

- nanoparticles derived from the cyanobacterium *Oscillatoria limnetica*. *Nature. Sci Rep*, (2019) 13071.
- 16 Gangula A, Podila R, Ramakrishna M, Karanam L, Janardhana C & Rao AM, Catalytic Reduction of 4-nitrophenol Using Biogenic Gold and Silver Nanoparticles Derived From *Breynia hamnoides*. *Langmuir*, 27 (2011) 15268.
 - 17 Wunder S, Lu Y, Albrecht M & Ballauff M, Catalytic activity of faceted gold nanoparticles studied by a model reaction: Evidence for substrate-induced surface restructuring. *ACS Catalysis*, 1 (2011) 908.
 - 18 Slavin YN, Asnis J, Häfeli UO & Bach H, Metal nanoparticles: understanding the mechanisms behind antibacterial activity. *J Nanobiotech*, 15(2017) 65.
 - 19 Ramamurthy C, Padma M, Mareeswaran R, Suyavaran A, Kumar MS, Premkumar K & Thirunavukkarasu C, The extra cellular synthesis of gold and silver nanoparticles and their free radical scavenging and antibacterial properties. *Colloids Surf B Biointerfaces*, 102 (2013) 808.
 - 20 Abbaszadegan A, Ghahramani Y, Gholami A, Hemmateenejad B, Dorostkar S, Nabavizadeh M & Sharghi H, The effect of charge at the surface of silver nanoparticles on antimicrobial activity against gram-positive and gram-negative bacteria: A preliminary study. *J Nanomater*, 16 (2015) 53.
 - 21 Qing Y, Cheng L, Li R, Liu G, Zhang Y, Tang X, Wang J, Liu H & Qin Y, Potential antibacterial mechanism of silver nanoparticles and the optimization of orthopedic implants by advanced modification technologies. *Int J Nanomed*, 13 (2018) 3311.
 - 22 Brunner TJ, Wick P, Manser P, Spohn P, Grass RN, Limbach LK, Bruinink A & Stark WJ, *In vitro* cytotoxicity of oxide nanoparticles: comparison to asbestos, silica, and the effect of particle solubility. *Environ Sci Technol*, 40 (2006) 4374.
 - 23 Kailasa SK, Park TJ, Rohit JV & Koduru JR, Antimicrobial activity of silver nanoparticles. (*Nanoparticles in Pharmacotherapy, Elsevier*) 2019, 461.